Available online at www.sciencedirect.com
ScienceDirect
International Journal of Heat and Mass Transfer 50 (2007) 1155–1162
International Journal of HEAT and MASS TRANSFER
www.elsevier.com/locate/ijhmt

Orthotropic thermal conductivity effect on cylindrical pin fin heat transfer

Raj Bahadur [a,*], Avram Bar-Cohen [b]

[a] Intel Corporation, Chandler, AZ 85226, USA
[b] Department of Mechanical Engineering, University of Maryland, College park, MD 20742, USA

Received 18 January 2005; received in revised form 19 April 2006
Available online 12 December 2006

Abstract

Analytical equations for temperature distribution and heat transfer rate from a cylindrical pin fin with orthotropic thermal conductivity, encountered in the use of thermally enhanced polymer composites, are derived and validated using detailed finite-element results. The thermal performance of such fins was found to depart from the classical fin solution with increasing radial conductivity-based Biot number. The in depth analysis of developed orthotropic axi-symmetric pin fin temperature and heat transfer rate equation is carried out to better understand the heat flow rate in such fins.

Keywords: Orthotropic thermal conductivity; Biot number; Pin fin heat transfer; Polymer composites; Carbon fiber; Fin optimization; Heat sink

1. Introduction

Recent advances in polymer composites, using carbon fiber [1], and graphite fillers [2] to increase the thermal conductivity, have made such materials viable alternatives to conventional metals in the design and fabrication of heat sinks and heat exchangers [see in Table 1]. Ongoing research into the use of carbon nanotubes (CNT's) [3] in epoxy matrixes may yield further improvements in such polymer composites. In addition to the manufacturing advantages offered by such moldable, high thermal conductivity composites, their relatively low density can provide a significant weight reduction and require less energy [4] for formation and fabrication than copper and aluminum, yielding an important contribution to sustainability.

Conventional polymers can be expected to display thermal conductivities in the range of 0.15–0.5 W/mK, but with the addition of high thermal conductivity continuous carbon fibers these composites can reach thermal conductivities of 300 W/mK in the fiber axis direction, as shown in Table 1. They display far lower thermal conductivities in the orthogonal (perpendicular to fiber axis) direction, with values that are as much as two orders of magnitude lower at 3 W/m K. Use of pitch based discontinuous fibers results in axial conductivity up to 100 W/m K and radial conductivity as low as the polymer conductivity of 0.4 W/m K.

Although numerous pin fin analyses exist in the literature [5–17], including the derivation of temperature and heat flow equations for two-dimensional isotropic pin fins [9,12], the impact of orthotropic thermal conductivity on the thermal performance of polymer composite fins has yet to be established. Failure to properly account for the role of orthotropy could limit the thermal designer's ability to predict and optimize the thermal performance of such polymer composite fins and heat sinks.

Classical fin, or extended surface, thermal analysis is based on the Murray-Gardener [5] assumptions, which – along with other assumptions – neglect the presence of radial temperature gradients in the fin and anisotropy in the fin material. It might be anticipated that for low Biot Number fins, signifying fins that are nearly isothermal in the radial direction, the classical relations would apply.

* Corresponding author.
E-mail address: rajbkunwar77@gmail.com (R. Bahadur).

0017-9310/$ - see front matter © 2006 Published by Elsevier Ltd.
doi:10.1016/j.ijheatmasstransfer.2006.04.025

Nomenclature

A	area (m^2)	λ	eigenvalues
Bi	Biot number, hR/k	σ	standard deviation
h	heat transfer coefficient (W/m^2 K)		
H	pin fin height (m)	*Subscripts and superscripts*	
J	Bessel function	a	ambient
k	thermal conductivity (W/m K)	b	fin base
k^*	fin conductivity ratio, k_r/k_z	c	cross section
m	fin parameter, $(2h/kR)^{1/2}$	gm	geometric mean, $(k_rk_z)^{1/2}$
q	heat flow rate (W)	hm	harmonic mean $(2k_rk_z)/(k_r+k_z)$
q^*	heat flow parameter, $q/k\theta_bR$	n	number
R	pin fin radius (m)	r	radial
T	temperature (K)	z	axial
r, z	polar coordinates (m)	‘	correction
γ	aspect ratio, $\gamma = H/R$	0	zero order
η	fin efficiency	1	1st order
θ	$T - T_a$		

Alternately, for large *Bi* fins with significant radial gradients, fin thermal performance can be expected to depart from the classical relations. This behavior may be observed in Fig. 1, showing a comparison between fin heat transfer rates obtained with an analytical two-dimensional isotropic solution [9,12,21] and values predicted by the classical and modified classical [8] relations. It may be seen that isotropic pin fin heat transfer rates can be determined using the classical pin fin equations [6,7] only up to Biot numbers of approximately 0.9 with less than a 10% discrepancy compared to two-dimensional isotropic solution. The Aparecido and Cotta modified 1D relation [8] extends this agreement up to Biot numbers of 4 or 5 with a 10–15% discrepancy. However, beyond these Biot values the classical 1D formulation over-predicts and the modified 1D equation under-predicts the two-dimensional pin fin cooling rate [9].

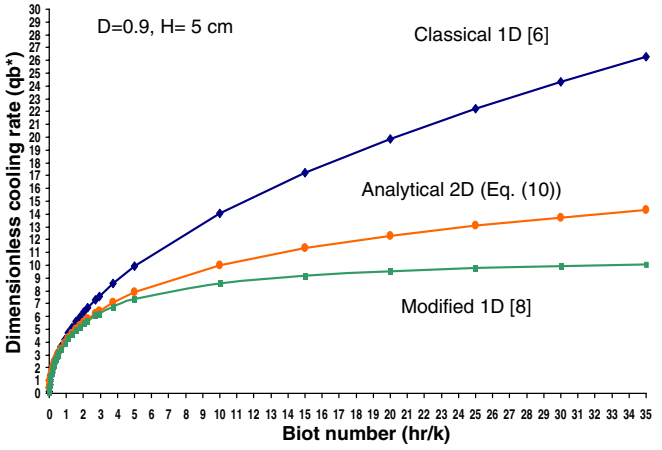

Fig. 1. Variation of non-dimensional isotropic pin fin cooling rate with radial Biot number ($H = 50$ mm, $D = 9$ mm).

In order to provide a context for the wide range of Biot numbers, consider a 2.2×10^{-6} m^3 (2.2 cm^3) polymer pin fin operating at 80% efficiency. When subjected to a typical forced convection heat transfer coefficient of 25 W/m^2 K, an unenhanced polymer [18,19] pin fin with a thermal conductivity of 0.3 W/m K will have a 10 mm radius and 7 mm height, yielding a *Bi* of 0.83. This same volume and material fin cooled by water, with an ‘*h*’ of 1000 W/m^2 K, results in optimum (80% efficiency) fin radius of 22 mm and 1.45 cm height and display a Biot number of 73. Alternatively, the *Bi* of a 2.2 cm^3 fin made of enhanced polymer with a conductivity of 3 W/m K and cooled by a 25 W/m^2 K heat transfer coefficient has 6.25 mm radius and

Table 1
Polymer composite properties

Filler	Matrix	Parallel to fibers (W/m K)	Normal to fibers (W/m K)	Density (g/cc)	Wt. (%) filler
Continuous carbon fiber	Polymer [1]	330	3–10	1.8	NA
Discontinuous carbon fiber	Polymer [1]	10–100	3–10	1.7	NA
Graphite	Epoxy [2]	370	6.5	1.94	NA
Single walled nanotubes	Epoxy [3]	0.5	NA	NA	1
Thermal graph DKD X	Lexan [20] HF110-11N	8	0.6	1.38	30
Thermal graph DKD X	Lexan [20] HF110-11N	11.4	0.74	1.46	40
Thermocarb CF300	Zytel 101 [20] NC010	1.1	0.4	1.17	5
Short carbon fiber	PPS [21]	15	4	1.7	80

1.8 cm height, yielding *Bi* of 0.052. It may, therefore, be expected that the performance of unenhanced, isotropic air cooled fins and enhanced water-cooled fins will display some significant departures from the classical predictions. On the other hand, for enhanced polymer fins used in air-cooled applications, it would appear that reasonably accurate results can be obtained using the classical 1D solution for all but the highest heat transfer coefficients.

1.1. Temperature profiles

The observed discrepancies at progressively larger *Bi* derive from the inability of the 1D formulation to accurately capture the radial temperature gradients that occur even in an isotropic pin fin. These gradients are accentuated by low thermal conductivity, large radius, and high heat transfer coefficients. This behavior can be seen in Fig. 2(a) and (b) that display, side by side, the one-dimensional [6] and two-dimensional [12] isotropic temperature distributions for a 9 mm radius and 50 mm high polymer fin with a thermal conductivity of 1 W/m K and a radial Biot number of 4.5. The fin has a constant base temperature of 95 °C and is exposed to an air convective heat transfer coefficient of 500 W/m^2 K in a 45 °C ambient temperature. The classical 1D solution by assumption produces isotherms that are parallel to the pin fin base and display no radial temperature variation (Fig. 2(a)). However, the more rigorous 2D solution, results in isotherms that, at *Bi* number of 4.5, are radially parabolic (Fig. 2(b)).

As a consequence of these different temperature profiles, the 1D solution for the specified pin fin configuration overpredicts the cooling rate (4.24 W) by 24% compared to the value predicted by the more rigorous 2D relation (3.42 W). The use of orthotropic polymer composite pin fins, with lower radial thermal conductivity than axial thermal conductivity, can be expected to lead to much larger radial temperature gradients than experienced in isotropic fins and, consequently, to greater deviations from the classical 1D fin solutions than seen in this example. If these newly available composite materials are to be successfully used for fins and heat sinks it is, thus, imperative that the effect of thermal orthotropy be incorporated into the thermal analysis and design of such orthotropic pin fins.

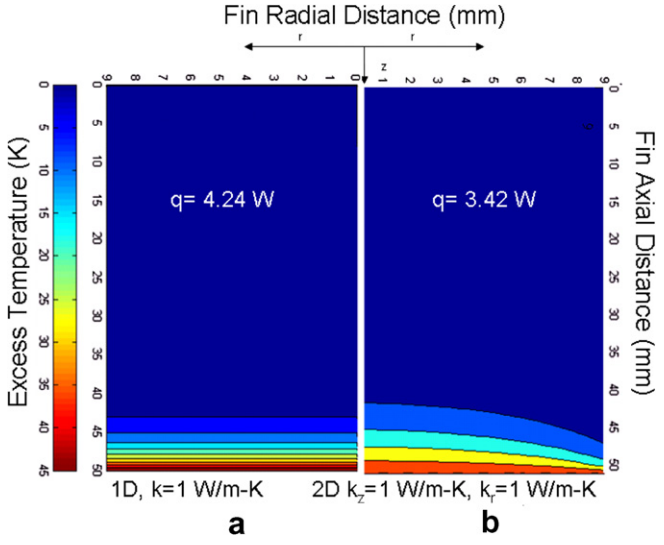

Fig. 2. Analytical excess temperature profile for an orthotropic low conductivity pin fin (a) 1D temperature field and (b) 2D temperature field.

2. Orthotropic pin fin – detailed model

2.1. Analysis

For steady state heat conduction in a radially symmetric, orthotropic fin with no internal heat generation and with θ defined as the fin excess temperature, i.e., $\theta = T - T_a$, the energy equation can be expressed in cylindrical coordinates, as:

$$k_r \frac{\partial^2 \theta}{\partial r^2} + k_r \frac{1}{r} \frac{\partial \theta}{\partial r} + k_z \frac{\partial^2 \theta}{\partial z^2} = 0. \tag{1}$$

Solution of this equation is sought under the following boundary conditions (referring to Fig. 3):

a. Symmetry boundary condition at the fin center line

$$r = 0 \quad \frac{\partial \theta}{\partial r} = 0. \tag{2}$$

b. Uniform and non-zero heat transfer coefficient at the fin tip

$$z = 0 \quad k_z \frac{\partial \theta}{\partial z} = h\theta. \tag{3}$$

c. Uniform heat transfer coefficient at fin surface

$$r = R \quad -k_r \frac{\partial \theta}{\partial r} = h\theta. \tag{4}$$

d. Fixed fin base excess temperature

$$z = H \quad \theta = \theta_b. \tag{5}$$

The governing equation for the fin excess temperature, Eq. (1), is homogeneous and the method of separation of

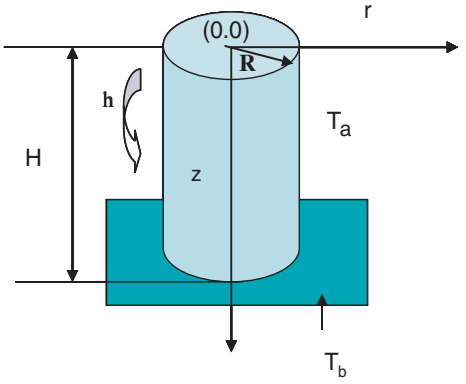

Fig. 3. Pin fin coordinates.

variables can be applied to its solution. Carrying out the separation of variables and obtaining the needed coefficients using orthogonality of the Bessel functions and utilizing the stated boundary conditions in Eqs. (2) and (3), the radial and axial variation of the pin fin excess temperature, $\theta(r,z)$ is found as [21]:

$$\theta(r,z) = 2\theta_b \sum_{n=1}^{\infty} \frac{\lambda_n J_1(\lambda_n) J_0\left(\lambda_n \frac{r}{R}\right)}{J_0^2(\lambda_n)[\lambda_n^2 + Bi_r^2]} x \times \frac{\left[1 + \exp\left(-2\left[\lambda_n (k^*)^{1/2} z/R + \tanh^{-1}\left(\frac{Bi_{gm}}{\lambda_n}\right)\right]\right)\right]}{\left[1 + \exp\left(-2\left[\lambda_n (k^*)^{1/2}\gamma + \tanh^{-1}\left(\frac{Bi_{gm}}{\lambda_n}\right)\right]\right)\right]} \times \exp(-\lambda_n (k^*)^{1/2}(H-z)/R) \quad (6)$$

Heat flow in such an orthotropic fin can be determined by applying Fourier's Law at the base of the fin. Thus, differentiation of Eq. (6) and evaluation of the temperature gradient at $z = H$, yields the relation for a fin heat flow, q_b, as [21]:

$$q_b = 4\pi k_z \theta_b R (k^*)^{1/2} x \sum_{n=1}^{\infty} \frac{Bi_r^2}{\lambda_n[\lambda_n^2 + Bi_r^2]} \times \frac{\left[1 - \exp\left(-2\left[\lambda_n \gamma (k^*)^{1/2} + \tanh^{-1}\left(\frac{Bi_{gm}}{\lambda_n}\right)\right]\right)\right]}{\left[1 + \exp\left(-2\left[\lambda_n \gamma (k^*)^{1/2} + \tanh^{-1}\left(\frac{Bi_{gm}}{\lambda_n}\right)\right]\right)\right]} \quad (7)$$

The eigenvalues for both Eqs. (6) and (7) are found by using the boundary condition expressed by Eq. (3) to obtain the following eigenvalue equation:

$$J_1(\lambda_n) = \frac{Bi_r}{\lambda_n} J_0(\lambda_n) \quad (8)$$

In order to conform to classical form, the exponential terms in Eq. (7) can be converted to hyperbolic tangents, yielding:

$$q_b = 4\pi k_z \theta_b R (k^*)^{1/2} \sum_{n=1}^{\infty} \frac{Bi_r^2}{\lambda_n[\lambda_n^2 + Bi_r^2]} \times \tanh\left[\lambda_n \gamma \left(\frac{k_r}{k_z}\right)^{1/2} + \tanh^{-1}\left(\frac{Bi_{gm}}{\lambda_n}\right)\right] \quad (9)$$

It is to be noted that eliminating the orthotropy contained in Eq. (7) by setting, $k_r = k_z = k$ and, hence $Bi_r = Bi_{gm} = Bi$, and $k^* = 1$ yields the 2D isotropic pin fin Eq. (10).

$$q_b = 4\pi k \theta_b R x \sum_{n=1}^{\infty} \frac{Bi_r^2}{\lambda_n[\lambda_n^2 + Bi_r^2]} \times \frac{\left[1 - \exp\left(-2\left[\lambda_n \gamma + \tanh^{-1}\left(\frac{Bi}{\lambda_n}\right)\right]\right)\right]}{\left[1 + \exp\left(-2\left[\lambda_n \gamma + \tanh^{-1}\left(\frac{Bi}{\lambda_n}\right)\right]\right)\right]} \quad (10)$$

Eq. (10) can be further rearranged [21], using Eq. (8), to take on the form of the two-dimensional isotropic relation appearing in the literature [9], i.e.,

$$q_b = 4\pi k \theta_b R x \sum_{n=1}^{\infty} \frac{\lambda_n [J_1(\lambda_n)]^2}{[\lambda_n^2 + Bi^2][J_0(\lambda_n)]^2} \times \frac{\lambda_n \sinh \lambda_n \gamma + Bi \cosh \lambda_n \gamma}{\lambda_n \cosh \lambda_n \gamma + Bi \sinh \lambda_n \lambda} \quad (11)$$

3. Orthotropic pin fin results

3.1. Analytical/numerical comparison

Fig. 4 displays a comparison of the analytical and numerical converged results obtained using ANSYS 7.1 [21] for the heat flow from an orthotropic pin fin 5 cm in length and 0.9 cm in diameter, with an axial thermal conductivity of 20 W/m K, subjected to a heat transfer coefficient variation from 10 to 5000 W/m^2 K and a base excess temperature of 40 K. A total of 99 distinct data points are shown for three different thermal conductivity ratios, $k^* = 0.015$, 0.25, and 1, and radial Biot numbers varying from 0.01 to 15. The plot clearly indicates very strong agreement (standard deviation, $\sigma = 0.073$) between the analytical results obtained with Eq. (7) and the 3D FEM simulation results using ANSYS 7.1. The FEM simulation was performed with a free mesh of up to 100 000 solid 70 elements for various described boundary conditions [21].

3.2. Temperature profile

The impact of thermal orthotropy can be clearly seen in Fig. 5, showing a comparison of the temperature profile for an isotropic and orthotropic fin, respectively. The temperature distribution for a pin fin with an isotropic thermal conductivity of 11.4 W/m K obtained via the 2D isotropic relation, Eq. (10), is shown in Fig. 5(a). Fig. 5(b) displays the temperature field for a thermally enhanced, orthotropic polymer pin fin case depicted in Table 1 with an axial thermal conductivity 11.4 and 0.74 W/m K radial thermal

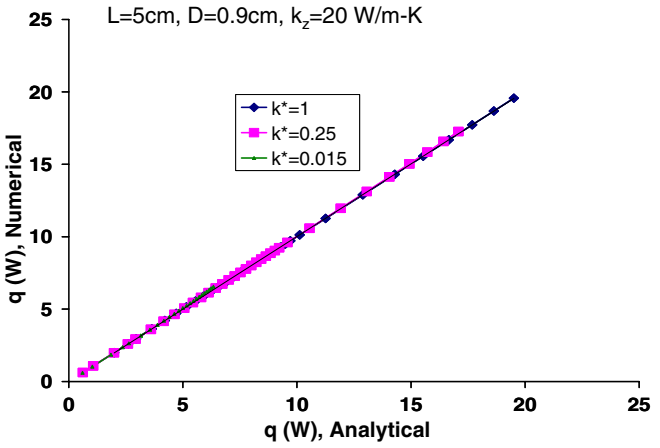

Fig. 4. Comparison of analytical and numerical orthotropic pin fin heat transfer rates – various conductivity ratios.

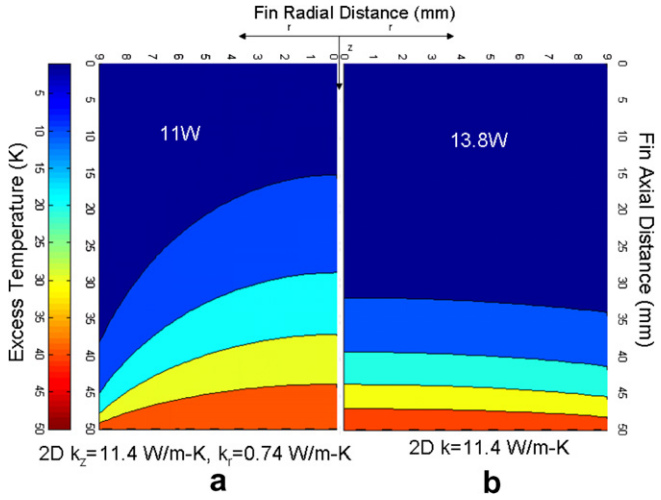

Fig. 5. Analytical excess temperature profile for a pin fin (a) Isotropic 2D – Eq. (10). (b) Orthotropic 2D – Eq. (7) ($H = 50$ mm, $D = 9$ mm, $h = 500$ W/m^2 K).

conductivity, obtained via Eq. (7). The pin fin in both cases has a 9 mm diameter and a 50 mm height; the fin base temperature is fixed at 95 °C in an ambient temperature of 45 °C, and is exposed to a uniform convective heat transfer coefficient of 500 W/m^2 K.

Fig. 5(b) clearly displays the two-dimensional character of the temperature distribution in an orthotropic pin fin, reflected in the far strong radial curvature of the isotherms throughout the fin volume than seen in the 2D isotropic temperature distribution Ignoring these increased radial temperature gradients by assuming isotropic axial conductivity leads to a 25% over prediction in the fin heat transfer rate (11 W versus 13.8 W). It is to be noted that application of the classical isotropic 1D fin analysis results in a further over prediction by some 5% and an erroneous heat transfer rate of 14.3 W for this geometry and operating conditions.

3.3. Thermal conductivity

Fig. 6 depicts the relatively weak, though complex, cooling rate dependence on the radial thermal conductivity, showing the cooling rate to increase linearly at relatively small values of k_r, followed by a gentle asymptotic rise over a large range of k_r values, for each value of k_z. Despite the complex functional dependence of q_b on k_r in Eq. (9), this behavior may well reflect the presence of k_r in the argument of the hyperbolic tangent function in the summation of eigenvalued terms. For the conditions studied numerically, the asymptotic domain appears to begin at progressively higher k_r values as the axial thermal conductivity value increases, transitioning to the asymptotic plateau at a radial thermal conductivity approximately one tenth of the axial thermal conductivity value. Thus for $k_z = 300$ W/m K the asymptotic transition occurs in the vicinity of $k_r = 30$ W/m K, while for an axial thermal conductivity of 30 W/m K, the asymptotic zone begins at $k_r = 3$ W/m K. The fin heat transfer rate follows an approximately square root dependence on axial conductivity as it increases from 0.3 to 300 W/m K.

3.4. Conductivity ratios

The effect of the thermal conductivity ratio on the pin fin cooling rate is depicted in Fig. 7 for the previously described case. In general the fin heat transfer rate increases with k^* and asymptotically approaches the limit associated with the classical 1D relation. For the lowest heat transfer coefficient studied (10 W/m^2 K), the improvement is nearly zero, while for the highest heat transfer coefficient (5000 W/m^2 K), a four-fold improvement is attained. The asymptotic limit is reached at k^* values of approximately unity, though for the high heat transfer coefficients that the fin could experience in water cooled heat exchangers [18] ($h = 5000$ W/m^2 K) the cooling rate continue to improve up to k^* values of 4.

The results shown in Fig. 8 for variable fin height and for a fixed heat transfer coefficient of 100 W/m^2 K, displaying the strong effect on the cooling rate of k^* values below unity and a progressively weaker effect for larger values of k^*, reinforces this conclusion. As the conductivity ratio increases, the radial temperature gradients diminish and

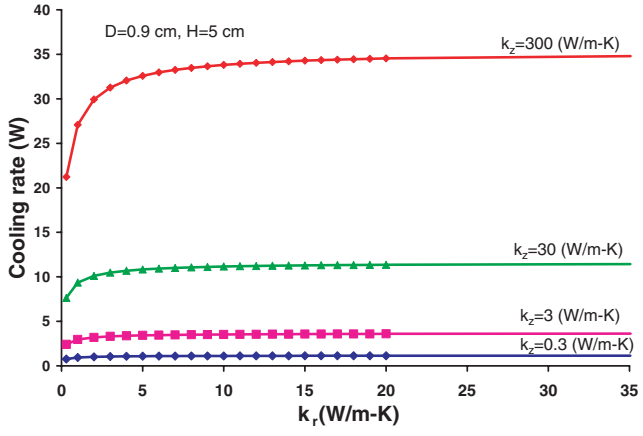

Fig. 6. Orthotropic pin fin cooling rate variation with radial and axial thermal conductivity – Eq. (9).

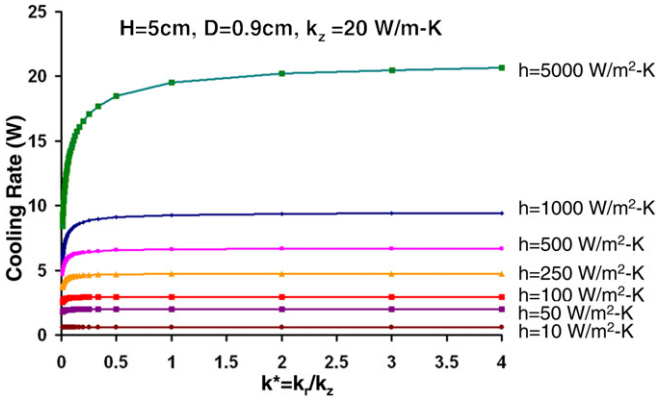

Fig. 7. Orthotropic pin fin cooling rate variation with thermal anisotropy – Eq. (9).

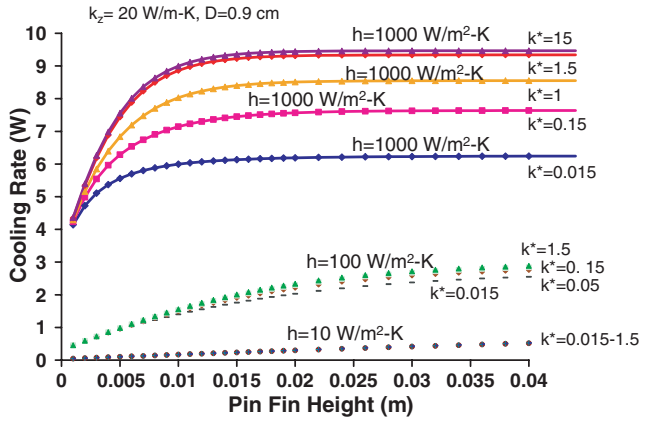

Fig. 8. Orthotropic pin fin cooling rate variation with fin height – Eq. (9).

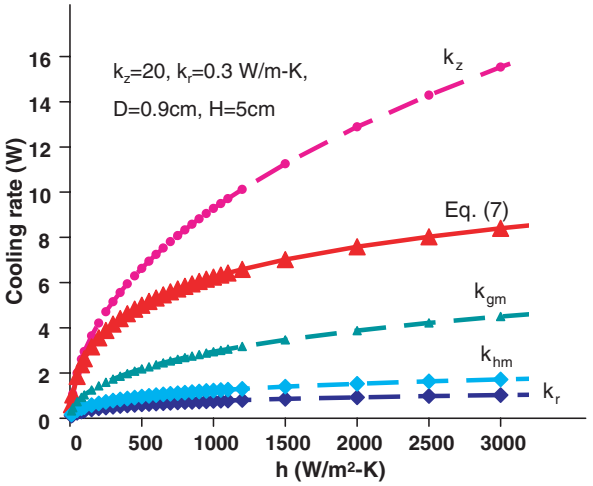

Fig. 9. Orthotropic pin fin cooling rate based on 1D model with effective thermal conductivities.

at k^* of unity or greater the heat transfer rate of this nearly radially-isothermal fin indeed should approach the heat transfer rates obtained from the classical 1D relation.

3.5. Fin height

The variation of the pin fin cooling rate with fin height, for a fixed axial thermal conductivity of 20 W/m K in an isothermal medium with a fixed heat transfer coefficient of 1000 W/m^2 K, is shown in Fig. 8. Interestingly, the variation with height – at conductivity ratios of unity as well as higher and lower values – mimics the asymptotic approach (typically hyperbolic tangent variation) to the maximum fin heat transfer rate found in the classical 1D pin fin solution. This behavior reflects the appearance of the fin height in the argument of the hyperbolic tangent inside the eigenvalued summation in Eq. (9). For a pin fin with fixed axial 20 W/m K and diameter of 9 mm, this optimum fin height is relatively constant at 0.015 m for a fixed heat transfer coefficient 1000 W/m^2 K over a broad conductivity ratio range obtained by varying radial thermal conductivity. The relatively weak dependence of the optimum pin fin height on the conductivity ratio has been further verified for heat transfer coefficients of 10 and 100 W/m^2 K, as shown in Fig. 8.

3.6. Effective conductivity

In the interest of streamlined thermal design, it is tempting to explore the potential for capturing the orthotropic effect through the use of an "effective" thermal conductivity in the classical 1D relation. Fig. 9 displays the cooling rates obtained using Eq. (7) for a single orthotropic pin fin of diameter 9 mm, fin height 50 mm, and a conductivity ratio of 60, subjected to a range of heat transfer coefficients and using several alternative definitions of "effective" thermal conductivity .

Examining Fig. 9, it is to be noted that the use of an effective thermal conductivity value based on the axial conductivity alone, as well as on the harmonic mean (0.6 W/m K) or geometric mean (2.45 W/m K) of k_r and k_z, or the radial conductivity alone, is incapable of predicting – even approximately – the cooling rate of the orthotropic fin over the broad range of heat transfer coefficients studied. However, for air-cooling heat transfer coefficients up to approximately 70 W/m^2 K, use of the axial thermal conductivity does provide a predictive accuracy to within 8%.

Moreover, even when the two-dimensional isotropic relation is used (Eq. 10), Fig. 10 reveals that none of the effective single thermal conductivity values can be used to accurately predicts the orthotropic pin fin cooling rate, for heat transfer coefficients above 70 W/m^2 K. For h values of about 80 W/m^2 K the 2D isotropic prediction shows an approximately 10% discrepancy, which grows to 110% at 1500 W/m^2 K, relative to the 2D orthotropic results using Eq. (9).

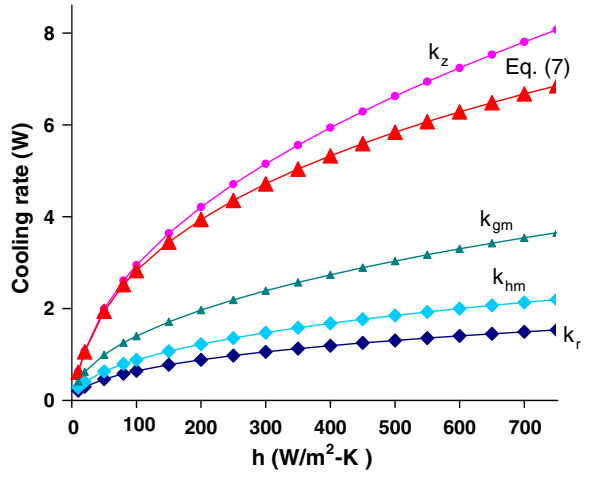

Fig. 10. Orthotropic pin fin cooling rate based on isotropic 2D relation with effective thermal conductivities.

4. Approximate orthotropic pin fin relations

4.1. Tip insulated fin

For typical pin fin geometries, fin tip area is a small fraction of the total wetted area. Therefore it is possible to approximate fin heat transfer by assuming negligible heat transfer from the pin fin tip. Setting $\partial\theta/\partial z$ to zero in Eq. (3) at the fin tip, and repeating the analysis described above, the total heat transfer rate from the lateral surface area of a tip-insulated pin fin is found to be expressible as

$$q_b = -4\pi k_z \theta_b R (k^*)^{1/2} \sum_{n=1}^{100} \frac{Bi_r^2}{\lambda_n [\lambda_n^2 + Bi_r^2]} \times \tanh\left(\lambda_n \left(\frac{k_r}{k_z}\right)^{1/2} \gamma\right). \quad (12)$$

Using a modified fin height which includes the tip area, i.e., adding one quarter of the pin diameter to pin fin height [7], in Eq. (12) increases the accuracy of this relation.

Fig. 11 displays a comparison between the orthotropic pin fin cooling rates, calculated using Eq. (12) with modified pin fin height, spanning aspect ratios (H/R) of 3-100, thermal conductivity ratios (k^*) from 0.015 to 1, and heat transfer coefficients ranging from 10 to 5000 W/m^2 K, for a total of 547 different cases. The largest discrepancy observed was 3.7%, for the lowest fin aspect ratio of 3, the thermal conductivity ratio of 0.05, and the highest considered heat transfer coefficient of 5000 W/m^2 K. As anticipated, the error associated with the simplified formulation of Eq. (12) decreases monotonically with increasing aspect ratio and conductivity ratio.

4.2. Domain-specific relations

Below Biot number of 0.4 using 1D classical solution with axial high thermal conductivity value provides inaccuracy in heat flow rate prediction within 5%. For radial Biot Numbers greater than 0.4 combined with describe orthotropic thermal conductivity values, the cooling rates have been found to depart significantly from the classical 1D isotropic conductivity solution. A major limitation in the use of the previously derived Eq. (9) to determine the orthotropic pin fin heat transfer rate is the need for calculating and summing a series of eigenvalues. Based on an extensive parametric study, it has, however, been found possible to represent the orthotropic effects with far simpler equations for each of two distinct heat transfer domains.

For $0.4 \leqslant Bi \leqslant 2$, corresponding to aggressive air cooling or water cooled free convection scenarios, Eq. (13) was found to offer results within 5% of the eigenvalue based solution, Eq. (9).

$$q = -4\pi k_z \theta_b R (k^*)^{1/2} (0.1333 \ln(Bi_r) + 0.3325) \times \tanh[(0.476 \ln(Bi_r) + 1.2632)(k^*)^{1/2}\gamma]. \quad (13)$$

Similarly for $2 \leqslant Bi \leqslant 35$, generally corresponding to forced convection water cooling, Eq. (14) was found to yield results well within 5% of the eigenvalue solution, Eq. (9), capturing the relatively prominent orthotropic effects in this domain.

$$q = -4\pi k_z \theta_b R (k^*)^{1/2} (0.2473 \ln(Bi_r) + 0.2456) \times \tanh[(0.156 \ln(Bi_r) + 1.8035)(k^*)^{1/2}\gamma]. \quad (14)$$

The comparison of the exact 2D orthotropic pin fin Eq. (9) with the proposed domain-specific Eq. (13) and Eq. (14), for the intermediate and high Bi range, respectively, is shown in Fig. 12, using a total of 560 data points. The aspect ratio ranges from 2.4 to 24 and radial Biot number ranges from 0.1 to 22.5. For aspect ratios of 2.4 and higher the values obtained via Eqs. (13) and (14) were found to fall within 5%, with the highest accuracy at the center of the prescribed radial Biot range and poorer agreement towards the limits. The highest discrepancy among considered cases in Fig. 12 is 5% obtained in case of a radial Biot number of

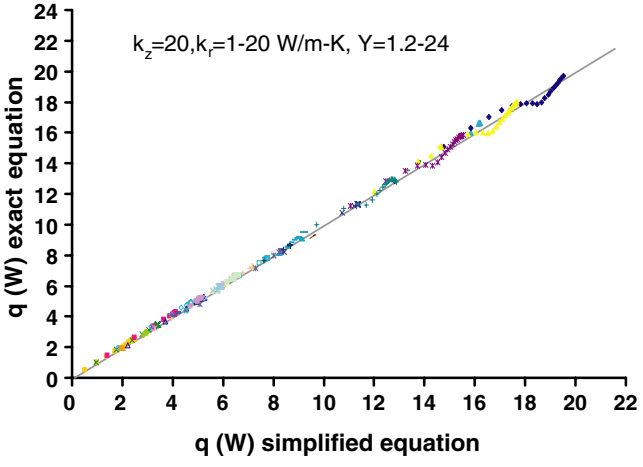

Fig. 11. Comparison of orthotropic cooling rates using insulated tip pin fin equation (Eq. (12)).

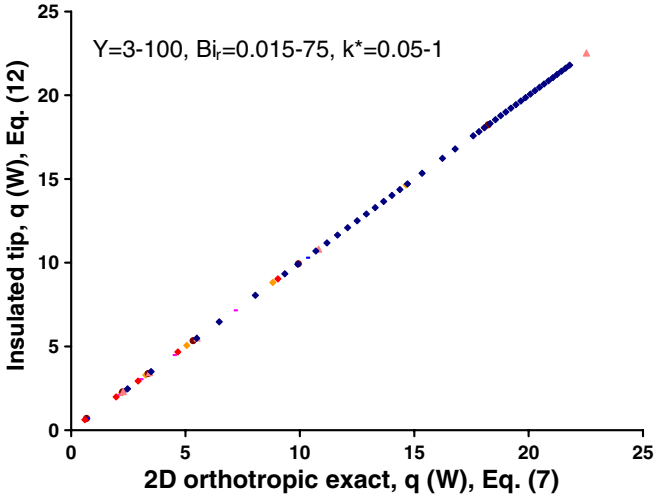

Fig. 12. Comparison of orthotropic pin fin heat transfer rates – 2D exact (Eq. (7)) and domain-specific relations (Eqs. (13) and (14)).

2 and aspect ratio of 2.4 using intermediate Eq. (13). Similarly, the highest discrepancy of 3.6% in using the high *Bi* range Eq. (14) is obtained at a radial Biot of 2.25 and aspect ratio of 11:1.

5. Conclusions

A closed form analytical solution for heat transfer from a cylindrical pin fin with orthotropic thermal conductivity is proposed. The resulting relation was numerically validated over a broad parametric range, including fin thermal conductivity ratios of 0.015–15, aspect ratios of 4–100, and radial Biot numbers of 0.0056–75. A tip-insulated approximation, yielding agreement to within 3.7% of the exact closed form equation for fin aspect ratios greater than 3, was also found.

For the parametric range studied, the impact of orthotropy on the pin fin heat transfer rate is found to increase with the radial Biot number and to decrease with increasing thermal conductivity ratio (radial/axial) and fin aspect ratio. Using these relations, it is determined that fin orthotropy does not materially affect the behavior of typical air-cooled fins. Alternatively, for heat transfer coefficients achievable with water cooling and conductivity ratios below 0.1, the fin heat transfer rate can fall more than 25% below the "classical" heat transfer rates.

Simplified, domain-specific pin fin heat flow solutions, convenient for thermal design and optimization of fin arrays, are proposed and shown to yield agreement to within 5% of the exact orthotropic relation.

References

[1] C. Zweben, Emerging high-volume commercial applications for thermally conductive carbon fibers, in: Proc. of the Sixth Int. business conference on the global outlook for carbon fiber, San Diego, California, November 5–7, 2003.

[2] Gary Shives et al., Comparative thermal performance evaluation of graphite/epoxy fin heat sinks, in: Proc. of intersociety for thermal conference (ITHERM), pp. 410–417, 2004.

[3] M.J. Biercuk, M.C. Laguno, M. Radosavljevic, J.K. Hyun, A.T. Johnsond, J.E. Fischer, Carbon nanotube composites for thermal management, Appl. Phys. Lett. 80 (2002) 2767–2769.

[4] R. Bahadur, A. Bar-Cohen, Thermal design and optimization of staggered polymer pin fin natural convection heat sinks, IEEE CPMT 28 (2) (2005) 238–246.

[5] K.A. Gardner, Efficiency of extended surfaces, Trans. ASME 67 (1945) 621–631.

[6] D.A. Kern, A.D. Kraus, Extended surface heat transfer, McGraw-Hill, New York, 1972, pp. 114–115.

[7] D.R. Harper, W.B. Brown, Mathematical equations for heat conduction in the fins in air cooled engines, NACA technical report, p. 188, 1922.

[8] J.B. Aparecido, R.M. Cotta, Improved one dimensional fin solutions, Heat Transfer Eng. 11 (1) (1990) 49–59.

[9] A.D. Kraus, A. Aziz, J. Welty, Extended Surface heat transfer, Wiley, New York, 2001, pp. 723–724.

[10] M.J. Levitsky, The criterion for the validity of the fin approximation, Int. J. Heat Mass Transfer 15 (1960) 1960–1963.

[11] M.N. Ozisik, Heat conduction, second ed., Wiley, New York, 1993.

[12] D. Poulikakos, Conduction heat transfer, Prentice Hall, Englewood Cliffs, NJ, 1994.

[13] B. Gebhart, Heat Conduction and mass diffusion, McGraw-Hill, New York, 1993.

[14] R.K. Irey, Error in one dimensional fin solution, J. Heat Transfer 90 (1968) 175–176.

[15] W. Lau, C.W. Tan, Errors in one dimensional heat transfer analysis in straight and annular fins, J. Heat Transfer 95 (November) (1973) 549–551.

[16] M.D. Mikhailov, M.N. Ozisik, Unified analysis and solutions of heat and mass diffusion, John Wiley, 1984.

[17] A. Aziz, H. Nguyen, Two dimensional performance of conducting–radiating fins of different profile shapes, Waerme and Stoffuebertrag 28 (1993) 481.

[18] J.H. Davidson, et al., Are plastic heat exchangers feasible for solar water heaters? Part I: A review of codes and standards and commercial products, in: Proc. of 1999 ASME Int. Solar Energy Conference. Maui, Hawaii, 1999.

[19] W. Liu, et al., Thermal and economic analysis of plastic heat exchangers for solar heating, in: Proc. of the 1999 American Solar Energy Conf., Portland, OR, 1999.

[20] E. Weber, Development and modeling of thermally conductive polymer/carbon composites, Ph.D. thesis, Chemical Engineering Department, Michigan Technological University, Michigan, 1999.

[21] R. Bahadur, Characterization, modeling and optimization of polymer composite pin fins, Ph.D. thesis, University of Maryland, College park, Maryland, 2005.